

Obliquity pacing of the late Pleistocene glacial terminations

Peter Huybers¹ & Carl Wunsch²

¹*Woods Hole Oceanographic Institution, Woods Hole, USA*

²*Massachusetts Institute of Technology, Cambridge, USA*

The timing of glacial/interglacial cycles at intervals of about 100,000y (100ky) is commonly attributed to control by Earth orbital configuration variations¹. This “pacemaker” hypothesis has inspired many models²⁻⁵, variously depending upon Earth obliquity, orbital eccentricity, and precessional fluctuations, with the latter usually emphasized. A contrasting hypothesis is that glacial cycles arise primarily because of random internal climate variability⁶⁻⁸. Progress requires distinguishing between the more than 30 models of the seven late Pleistocene glacial variations⁹. Here we present a formal test of the pacemaker hypothesis, focusing on the rapid deglaciation events known as terminations^{10,11}. The null hypothesis that glacial terminations are independent of obliquity is rejected at the 5% significance level. In contrast, for eccentricity and precession, the corresponding null-hypotheses are not rejected. The simplest inference, consistent with the observations, is that ice-sheets terminate every second (80ky) or third (120ky) obliquity cycle—at times of high obliquity—and similar to the original Milankovitch assumption¹². Simple stochastic and deterministic models are presented which describe the timing of the 100ky cycles of the late Pleistocene glacial terminations purely in terms of obliquity forcing.

To test whether the glacial variability is related to changes in Earth's astronomical configuration, we adopt a formal null-hypothesis (H_0) that glacial terminations are independent of obliquity variations, and the alternate hypothesis (H_1) that glacial terminations are paced by it. Our focus on obliquity is motivated by previous indications of nonlinear interactions between obliquity period and quasi-100ky glacial variability¹³, but we also make identical tests for pacing by precession and eccentricity. The test is focussed on glacial terminations because their magnitude and abruptness facilitate accurate identification.

Several obstacles must be overcome to distinguish between H_0 and H_1 . A major problem is the need to establish time controls on the glacial variability. Many studies estimate age by assuming a relationship between climate proxy variability and orbital forcing^{14,15}, but this approach assumes the validity of the hypothesis being tested. Instead, we use an age-model devoid of orbital assumptions and apply it to the leading empirical orthogonal function (EOF1) of ten well-resolved marine $\delta^{18}O$ records¹³, a proxy for ice-volume and ocean temperature (Fig 1a).

Most simple models of the late Pleistocene glacial cycles have at least four degrees of freedom², and some have as many as twelve³. Unsurprisingly then, the seven observed quasi-100ky glacial cycles are insufficient to distinguish between the skill of the various models¹⁶. Models with minimal degrees of freedom are necessary. Other requirements for a useful test include the ability to cope with noisy records, age-model uncertainty, and (possibly) nonlinear interactions. Here we test for stability in the phase of the orbital parameters during glacial terminations using *Rayleigh's R* (see Methods).

To proceed, we must estimate the probability distribution function associated with H_0 . Of the five estimation methods explored, the one adopted gives the highest critical value and thus makes H_0 the most difficult to reject — a modified random walk⁸ representing ice-volume variability,

$$V_{t+1} = V_t + \eta_t,$$

$$\text{if } V_t \geq T_o, \text{ terminate.} \quad (1)$$

This highly simplified model posits 1ky steps in ice-volume, V_t , of random length, η_t , independently drawn from a normal distribution with standard deviation $\sigma = 2$ and mean $\mu = 1$. The non-zero mean biases the Earth toward glaciation. Once V_t reaches a threshold, $T_o = 90$, a termination is triggered, and ice-volume is linearly reset to zero over 10ky. If the model were deterministic with $\sigma = 0$ and $\mu = 1$, glacial cycles would last exactly 100ky, but with $\sigma = 2$, glacial cycle duration is approximately normally distributed at 100 ± 20 ky, a spread consistent with observations¹¹. Initial ice-volume is randomly set between 0 and T_o with equal probability. From a Monte Carlo technique (see Methods), we find a critical value of $R = 0.60$.

The observed obliquity phases produce $R = 0.70$, and H_0 is rejected (Fig 1b). This rejection of H_0 is robust to all plausible reformulations of the test. Thus, the phase of obliquity has a statistically significant relationship with the timing of deglaciation. The mean phase at deglaciation is indistinguishable from zero and is associated with maxima in obliquity. We estimate the H_1 probability density function by assuming terminations always initiate at the same phase of obliquity, but that termination timing is subject to identification and age-model uncertainties (see Methods). The maximum likelihood value of H_1 is $R = 0.69$, very near the observed value, further supporting the conclusion that glacial terminations are paced by

variations in obliquity. Hypotheses not accounting for the obliquity pacing are unlikely to be correct.

Analogous hypothesis tests for precession and eccentricity produce different results (Fig 1c,d). Age-model uncertainty approaches half a precession cycle, so that the power of the precession test is negligible — even if present, precession pacing of the glacial cycles cannot be discerned. In the case of eccentricity, H_0 is not rejected using the random walk probability estimate (Eq 1), but is rejected using weaker formulations of the eccentricity null-hypothesis. The discrepancy arises because null-hypotheses which assume a glacial timescale of roughly 100ky (which seem more physical) tend to have higher R 's and are more difficult to reject. As the hypotheses of negligible influence of precession and eccentricity on the glacial terminations cannot be rejected, we adopt a minimalist strategy, retaining only obliquity to describe the glacial terminations.

From a physical standpoint, support for the obliquity control hypothesis also comes from the fact that maxima in obliquity cause annual average insolation anomalies of up to 10W/m^2 at high latitudes. Furthermore, the annual average and seasonal insolation redistributions associated with obliquity are hemispherically symmetric — as is the glacial variability to within a few thousand years^{17,18}. Finally, while obliquity control does not by itself address the question of why termination five is anomalously large, it does alleviate the marine isotope stage 11 problem² of explaining the initiation of termination five when eccentricity and precession amplitude are small.

But how does a forcing with a 40ky period pace the 100ky late Pleistocene glacial variability? One suggestion is that the phase and amplitude modulations of obliquity cause the

100ky variability⁴, but it is difficult to see the climatic significance of such modulations. Instead, we suggest that the climate state skips one or two obliquity beats prior to deglaciating, thus giving quantized glacial cycle durations of either 80 or 120ky. A speculative scenario is for increased obliquity to increase high-latitude insolation and cause heating of an ice-sheet, eventually warming the ice-bedrock interface. When the ice-sheet is thin, basal temperature and pressure are low¹⁹, and the obliquity heating has little effect — a skipped beat. But when the ice-sheet is thick, basal temperature and pressure are high¹⁹, and additional obliquity heating promotes basal melting. Enhanced lubrication of the ice-bedrock interface may trigger deglaciation by increasing ice-flux into the ocean or toward lower latitudes, as well as by increasing the thinning rate and causing inward migration of the ablation zone²⁰. Note that ~ 10 ky is required for surface heating to penetrate to the base of an ice-sheet¹⁹. Unlike precession, changes in obliquity are associated with sustained annual average changes in insolation^{21,22} and, thus, are more likely to cause basal warming. Furthermore, if climate was warmer during the early Pleistocene, terminations would be triggered more nearly every obliquity cycle, giving the observed smaller and more rapid glacial variability²³.

A simple system, consistent with the foregoing observations, is obtained by making the threshold in Eq 1 dependent on obliquity,

$$\begin{aligned}
 V_{t+1} &= V_t + \eta_t, \\
 &\text{if } V_t \geq T_o - a\bar{\theta}_t, \text{ terminate.}
 \end{aligned}
 \tag{2}$$

Here $\bar{\theta}_t$ is obliquity²⁴, normalized to zero mean and unit variance, with amplitude a . The time variable threshold makes it more likely for a termination to occur when obliquity is large. Both deterministic and stochastic variants of Eq 2 are offered to emphasize that such models are not

theories of climate change, but rather attempts at efficient kinematic descriptions of the data, and that different mechanisms can be consistent with the limited observational records.

To make the model deterministic, the ice-volume step-size in Eq 2 is fixed at $\eta = 1$. Setting $a = 15$, $T_o = 105$, and (initial ice-volume) $V_{(t=-700)} = 30$ provides a good description of the late Pleistocene glacial variability (Fig 2a). Many other parameterizations yield similar results — we choose this one because it is particularly simple. The model produces the correct timing of the glacial terminations (using termination 3a, not 3b) and has a squared-cross-correlation with $\delta^{18}O$ EOF1 of 0.65, an excellent fit considering there are only three adjustable parameters. (Parameters other than η could be adjusted instead.) For comparison, tuning other models having four² or twelve³ adjustable parameters yields a maximum squared-cross-correlations with EOF1 of 0.24 and 0.74 respectively²⁵. If skill is measured by squared-cross-correlation divided by the number of adjustable parameters, Eq 2 does more than three times as well.

A periodogram of the deterministic model results (Fig 2b) shows narrow-band concentrations of energy at the average 100ky period, the 41ky obliquity period, and at previously identified¹³ combination tones, $1/41-1/100=1/70$, $1/41+1/100=1/29$, and $1/41+2/100=1/23$ ky — in good agreement with the $\delta^{18}O$ EOF1 periodogram. The appearance of 1/23ky narrow-band energy, in the absence of precession band forcing, highlights the ambiguous origins of this energy band²². The model also has energy at 2/100ky, not visible in the observations. Note that the model produces an energetic background continuum consistent with the $\delta^{18}O$ periodogram even though it is deterministic.

For the stochastic case, η_t is defined to be normally distributed with $\sigma = 2$ and $\mu = 1$. Here η_t represents the unpredictable background weather and climate variability spanning all time scales out to the glacial/interglacial. All other parameter settings are kept the same as in the deterministic case. Now, Eq 2 resembles an order one autoregressive process. Such a process is known to well-describe the glacial variability, excepting runs associated with glacial terminations²⁶, here modeled using the threshold condition in Eq 2. The time between terminations in the stochastic model averages 100ky but has a tri-modal distribution with maxima at two (80ky), three (120ky), and four (160ky) obliquity cycles (Fig 2d). The observed durations between terminations are consistent with the dominant 80 and 120ky modes, but suggest that one would see 160ky glacial cycles, given a larger sample size. The R obtained by the stochastic model averages 0.85 (Fig 2e), higher than the observed $R = 0.70$, and as expected because of observational age-model error.

Deterministic and stochastic variants of Eq 2 thus both describe the late Pleistocene glacial variability. A description of the early Pleistocene variability²³ is obtained by lowering the termination threshold to $T_o = 40$, giving smaller amplitude terminations that occur more nearly every obliquity cycle. Alternatively, instead of specifying a parameter change, the mid-Pleistocene transition can be described using a chaotic model²⁵ (not shown) having spontaneous transitions between 40 and 100ky modes of glacial variability. With only seven cycles, it is unclear whether adequate data will ever be available to distinguish between stochastic, simple deterministic, and chaotic deterministic models of the glacial variability.

The simplest interpretation of our results is that during the Pleistocene Earth tends to a

glacial state (anthropogenic influences aside) and deglaciates near some, but not all, obliquity maxima. Obliquity control of the timing of deglaciation, probably in concert with a stochastic forcing, has several other consequences. These include inferences drawn from precession and eccentricity based models of glaciation²⁷, the hemispheric symmetry of glacial cycles, and the efficacy of age-model tuning of cores. These issues will be taken up elsewhere.

Methods

Rayleigh’s R is defined as²⁸

$$R = \frac{1}{N} \left| \sum_{n=1}^N \cos \phi_n + i \sin \phi_n \right|. \quad (3)$$

Here, ϕ_n is the phase of obliquity stroboscopically sampled at the n th glacial termination. The $|\cdot|$ indicate the magnitude, making R real and non-negative, with a maximum value of one when the phases are all equal. Relative to measures of phase coupling used to investigate other nonlinear interactions²⁹, Rayleigh’s R requires many fewer phases (roughly five) to test for phase stability²⁸.

To measure R between obliquity and the glacial cycles, we use $\delta^{18}O$ EOF1 and an age-model independent of orbital assumptions¹³ (Fig 1a). Such an independent age-model is important because even so-called minimal tuning strategies — using only a narrow-band of a climate record — tend to align the abrupt glacial terminations with a particular phase of the assumed forcing (as indicated by Monte Carlo simulations), thus biasing records towards H_1 .

The rate of change of EOF1 has a unimodal distribution with a long tail, indicative of rapid

melting. Terminations are defined to initiate when the rate of change in EOF1 first exceeds the two-standard deviation level. This criterion identifies each of the usual terminations^{10,11}, but two events in the termination 3 deglacial sequence, termed 3a and 3b for the younger and older events respectively. Additional rules could be added to exclude 3a or 3b, but this rejection seems ad hoc, and we use all eight termination events. Note, the timing of termination 3 predicted by the Paillard model³ also coincides with either event 3a or 3b, depending on slight changes in the parameterizations. Reassuringly, results are not sensitive to details of the test: either termination 3a or 3b can be excluded; termination times can be defined using the midpoint between the local minimum and maximum bracketing each termination; and individual benthic or planktic $\delta^{18}O$ records¹⁵ can be used in place of EOF1.

The probability density function (PDF) associated with H_0 is estimated using the modified random walk model (Eq 1). A realization of R is obtained by sampling the phase of obliquity at eight consecutive termination initiations, generated from Eq 1, and the PDF of H_0 is estimated by binning 10^4 such realization of R . Other methods are to assume a uniform phase distribution, use surrogate data techniques, or to derive statistics from ensemble runs of other models, but all these give PDF estimates which make H_0 more easily rejected and are therefore not used.

To estimate the PDF associated with H_1 , we assume that glacial terminations always occur at the same phase of obliquity, but that the phase observations are subject to identification and age-model error. A Monte Carlo technique is used where the timing of the glacial terminations are perturbed according to the estimated age uncertainties¹³ (these average ± 9 ky) and identification error (± 1 ky, the EOF1 sampling resolution). A realization of R is then computed using

the phase of obliquity at the perturbed ages, and 10^4 such realizations are binned to estimate the PDF of H_1 . We estimate the likelihood of correctly rejecting H_0 (i.e. the power of the obliquity test) to be 0.57. See the supplementary web information for a listing of the other pertinent data and statistics.

Bibliography

1. Hays, J., Imbrie, J. & Shackleton, N. Variations in the earth's orbit: Pacemaker of the ice ages. *Science* **194**, 1121–1132 (1976).
2. Imbrie, J. & Imbrie, J. Modeling the climatic response to orbital variations. *Science* **207**, 943–953 (1980).
3. Paillard, D. The timing of Pleistocene glaciations from a simple multiple-state climate model. *Nature* **391**, 378–391 (1998).
4. Liu, H. Insolation changes caused by combination of amplitude and frequency modulation of the obliquity. *Journal of Geophysical Research* **104**, 25197–25206 (1999).
5. Gildor, H. & Tziperman, E. Sea ice as the glacial cycles' climare switch: Role of seasonal and orbital forcing. *Paleoceanography* **15**, 605–615 (2000).
6. Saltzman, B. Stochastically-driven climatic fluctuations in the sea-ice, ocean temperature, co₂, feedback system. *Tellus* **34**, 97–112 (1982).
7. Pelletier, J. Coherence resonance and ice ages. *Journal of Geophysical Research* **108**, doi:10.1029/2002JD003120 (2003).

8. Wunsch, C. The spectral description of climate change including the 100ky energy. *Climate Dynamics* **20**, 353–363 (2003).
9. Saltzman, B. *Dynamical Paleoclimatology: Generalized Theory of Global Climate Change* (Academic Press, San Diego, 2002).
10. Broecker, W. Terminations. In Berger, A. & et. al. (eds.) *Milankovitch and climate, Part2*, 687–698 (D. Riedel, Hingham, 1984).
11. Raymo, M. E. The timing of major climate terminations. *Paleoceanography* **12**, 577–585 (1997).
12. Milankovitch, M. *Kanon der Erdbestrahlung und seine Anwendung auf das Eiszeitenproblem* (Royal Serbian Academy, Belgrade, 1941).
13. Huybers, P. & Wunsch, C. A depth-derived Pleistocene age-model: Uncertainty estimates, sedimentation variability, and nonlinear climate change. *Paleoceanography* **19**, doi:10.1029/2002PA000857 (2004).
14. Imbrie, J. *et al.* The orbital theory of Pleistocene climate: Support from a revised chronology of the marine delta 18 O record. In Berger, A. e. a. (ed.) *Milankovitch and Climate, Part 1*, 269–305 (D. Riedel Publishing Company, 1984).
15. Shackleton, N. J., Berger, A. & Peltier, W. R. An alternative astronomical calibration of the lower Pleistocene timescale based on ODP site 677. *Trans. R. Soc. Edinb.-Earth Sci.* **81**, 251–261 (1990).

16. Roe, G. & Allen, M. A comparison of competing explanations for the 100,000-yr ice age cycle. *Geophysical Research Letters* **26**, 2259–2262 (1999).
17. Blunier, T. & Brook, E. Timing of millennial-scale climate change in Antarctica and Greenland during the last glacial period. *Science* **291**, 109–112 (2001).
18. Wunsch, C. Greenland-Antarctic phase relations and millennial time-scale climate fluctuations in the Greenland cores. *Quaternary Science Reviews* **22**, 1631–1646 (2003).
19. Marshall, S. & Clark, P. Basal temperature evolution of North American ice sheets and implications for the 100-kyr cycle. *Geophysical Research Letters* **29**, doi:10.1029/2002GL015192 (2002).
20. Zwally, H. *et al.* Surface melt-induced acceleration of Greenland ice-sheet flow. *Science* **297**, 218–222 (2002).
21. Rubincam, D. Insolation in terms of earth's orbital parameters. *Theoretical Applied Climatology* **48**, 195–202 (1994).
22. Huybers, P. & Wunsch, C. Rectification and precession-period signals in the climate system. *Geophysical Research Letters* **30**, doi:10.1029/2003GL017875 (2003).
23. Raymo, M. & Nisancioglu, K. The 41 kyr world: Milankovitch's other unsolved mystery. *Paleoceanography* **18**, doi:10.1029/2002PA000791 (2003).
24. Berger, A. & Loutre, M. F. Astronomical solutions for paleoclimate studies over the last 3 million years. *Earth Planet. Sci. Lett.* **111**, 369–382 (1992).

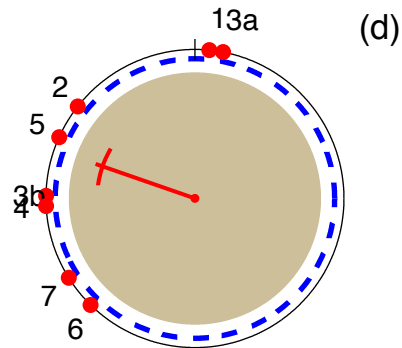
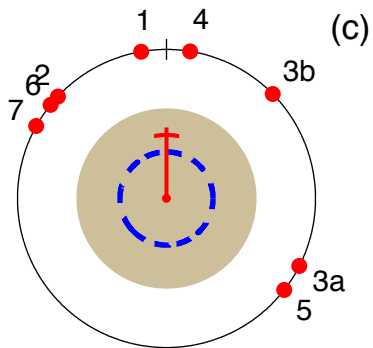
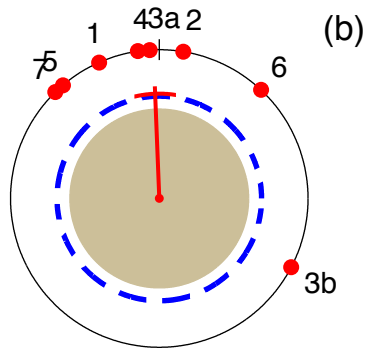
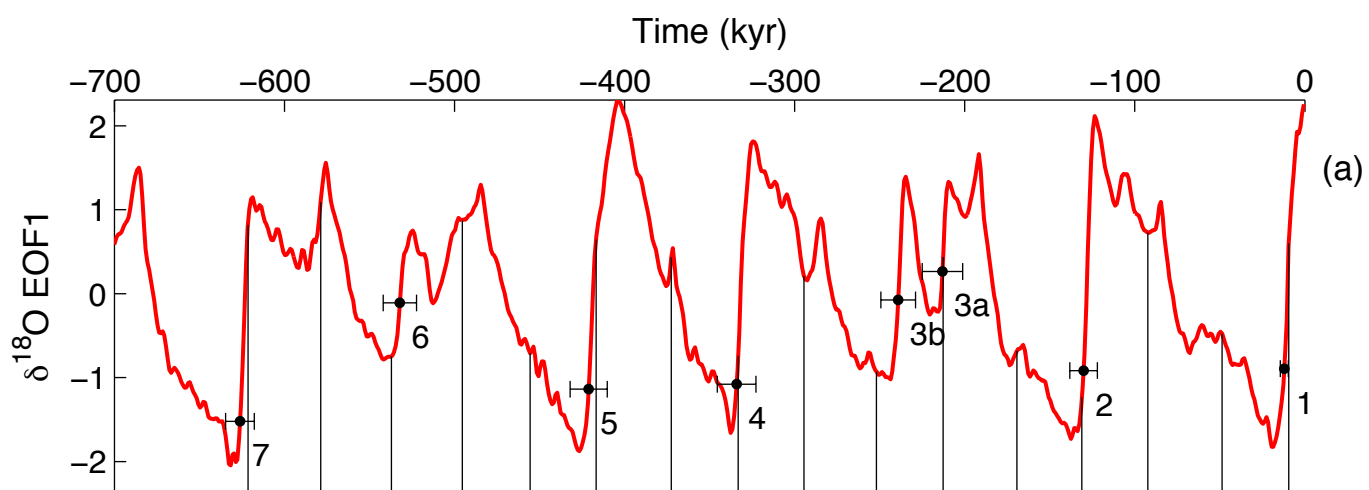
25. Huybers, P. *On the Origins of the Ice Ages: Insolation Forcing, Age Models, and Nonlinear Climate Change*. Ph.D. thesis, MIT (2004).
26. Wunsch, C. Quantitative estimate of the Milankovitch-forced contribution to observed quaternary climate change. *Quaternary Science Reviews* **23**, 1001–1012 (2004).
27. Ruddiman, W. F. Orbital insolation, ice volume, and greenhouse gases. *Quaternary Science Reviews* **22**, 1597–1622 (2003).
28. Upton, G. & Fingleton, B. *Spatial Data Analysis by Example*, vol. 2 (John Wiley and Sons, Chichester, 1989).
29. Rosenblum, M. & Pikovsky, A. Synchronization: from pendulum clocks to chaotic lasers and chemical oscillators. *Contemporary Physics* **44**, 401–416 (2003).
30. Schreiber, T. & Schmitz, A. Surrogate time series. *Physica D* **142**, 346–382 (2000).

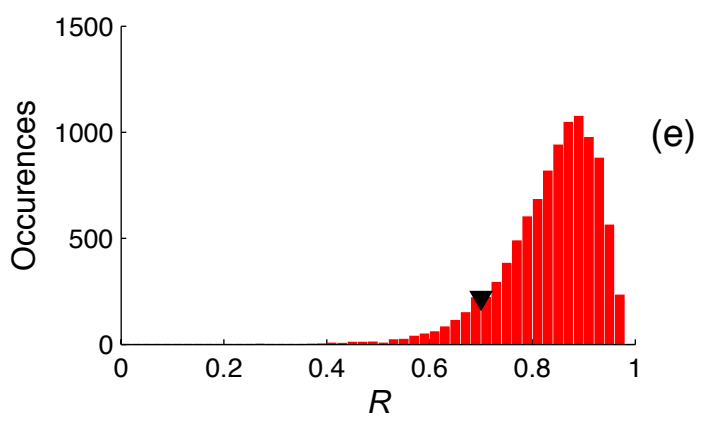
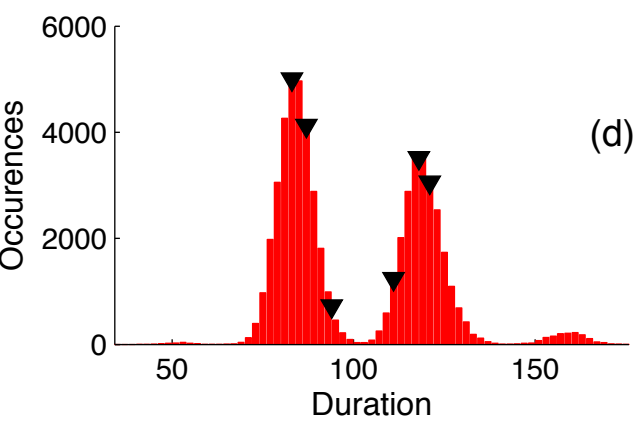
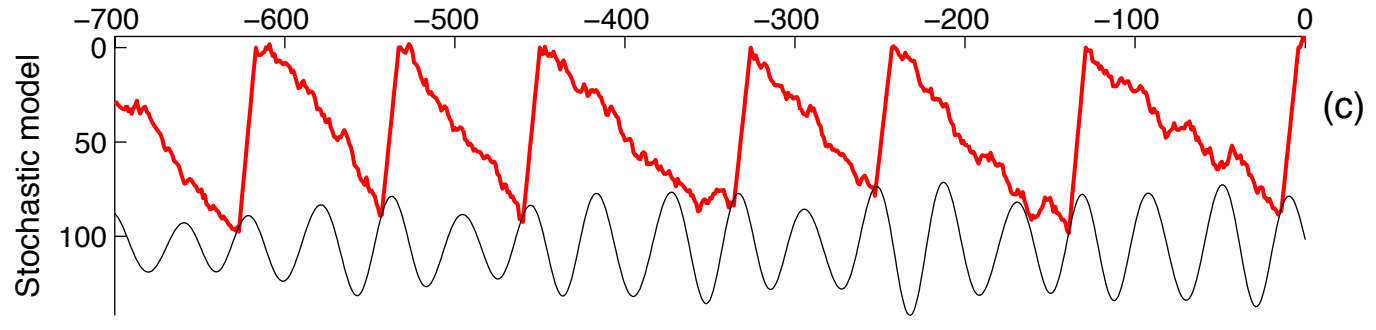
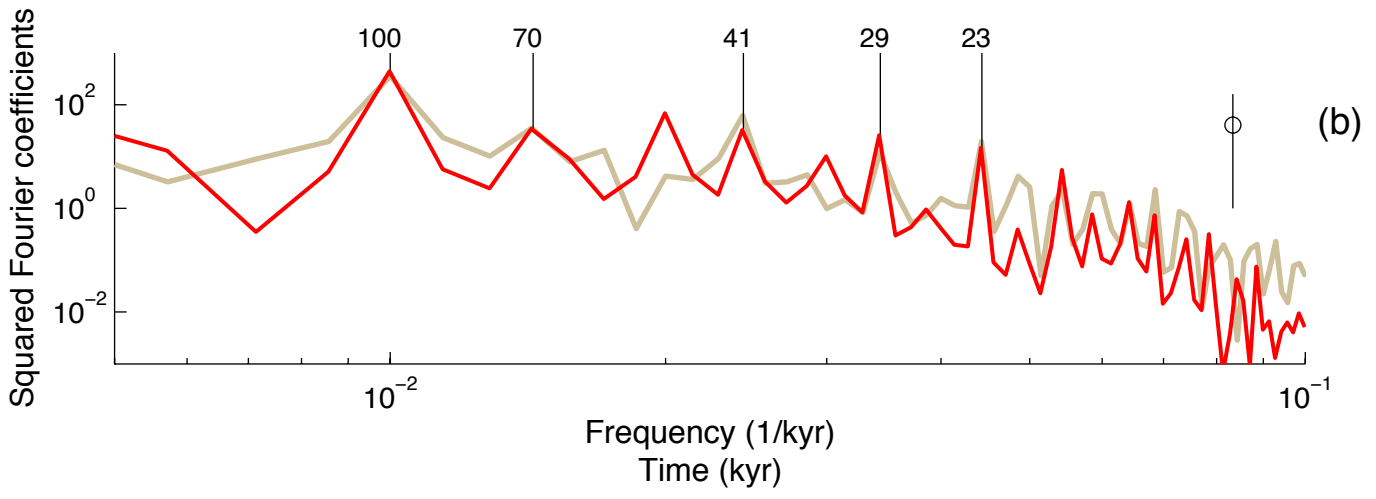
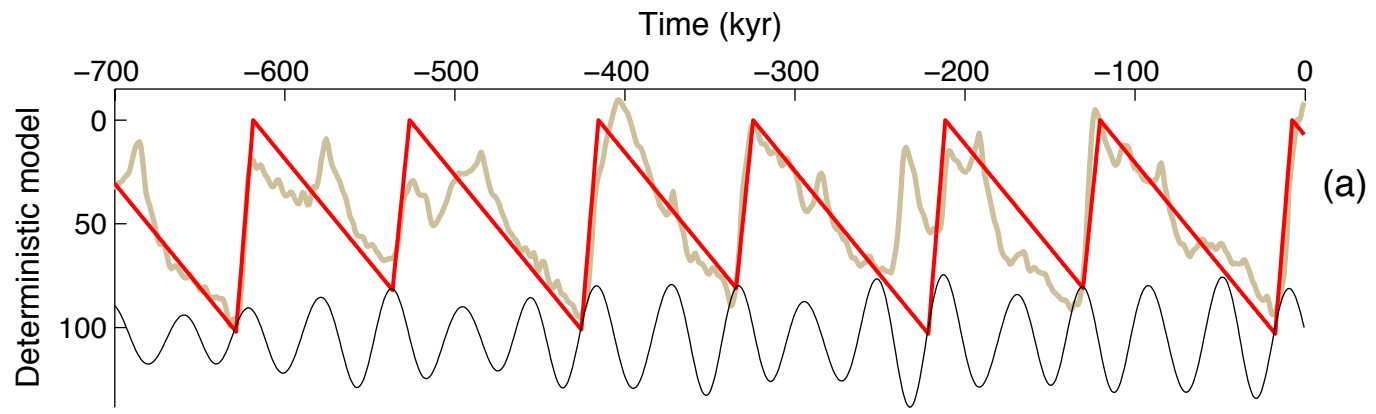
Acknowledgments. Useful comments were provided by E. Boyle, W. Curry, Tim Herbert, J. McManus, Felix Ng, M. Tingley, and G. Yang. PH is supported by the NOAA Postdoctoral Program in Climate and Global Change and CW in part by the National Ocean Partnership Program (ECCO).

Correspondence and requests for materials should be addressed to phuybers@whoi.edu.

Figure 1 The Rayleigh test for phase directionality. **a**, $\delta^{18}O$ EOF1 normalized so that negative values indicate more ice. Dots indicate onset of a termination and horizontal bars indicate one-standard-deviation age-model uncertainties¹³. Termination 3 is split between events 3a and 3b. Vertical lines indicate the time of maxima in obliquity. **b**, The obliquity phase (dots) sampled at each termination and plotted on a unit circle. The vector average has a magnitude, $R = 0.70$ (cross mark), exceeding the critical value, $c = 0.60$ (filled circle), so that H_0 is rejected. Furthermore, R is near H_1 's maximum likelihood value (dashed circle). The direction is indistinguishable from maximum obliquity (top of the circle). Analogous tests are made for **c** precession ($R = 0.43$, $c = 0.60$) and **d** eccentricity ($R = 0.66$, $c = 0.84$), but in neither case can the corresponding H_0 be rejected. See the supplementary web information for more details.

Figure 2 Deterministic and stochastic descriptions of the late Pleistocene glacial variability. **a** Deterministic model results (red) with an obliquity dependent threshold (black) plotted over EOF1 (brown). **b** Periodograms of the deterministic model results (red) and EOF1 (brown). Concentrations of energy are centered on the 1/41ky obliquity frequency and the 1/100ky glacial band; as well as combination tones at 1/70, 1/29, and 1/23ky. The approximate 95% confidence interval is indicated by the vertical bar at right. **c** A realization of the stochastic model. **d** Histogram of time between terminations, derived from many runs of the stochastic model. The observed duration between terminations (triangles, using termination 3a not 3b) coincide with the dominant 80 and 120ky modes. **e** Histogram of Rayleigh's R from the stochastic model with the observed obliquity value, $R=0.70$, indicated by the triangle.





huybers fig2